

A tunable fluorescence probe for superoxide anion detection during inflammation caused by *Treponema pallidum*

Weiqliang Lin^{a,†}, Jialin Huang^{a,†}, Shuang Guo^{a,†}, Meijiao Zhao^a, Xu Chen^c, Qiuping
Shang^a, Ruoyuan Zhang^a, Guangfu Liao^{b,*}, Judun Zheng^{a,*}, Yuhui Liao^{a,d,*}

^a Molecular Diagnosis and Treatment Center for Infectious Diseases, Dermatology Hospital, Southern Medical University, Guangzhou, 510091, P. R. China

^b College of Material Engineering, Fujian Agriculture and Forestry University, Fuzhou, 350002, P. R. China

^c Department of Infectious Disease, the Fifth Affiliated Hospital, Sun Yat-sen University, Zhuhai, 519000, P. R. China

^d NHC Key Laboratory of Metabolic Cardiovascular Diseases Research, Ningxia Key Laboratory of Vascular Injury and Repair Research, Ningxia Medical University, Yinchuan, 750004, P. R. China

† Electronic Supplementary Information (ESI) available.

‡ These authors contributed equally.

*Correspondence Authors

Yuhui Liao: E-mail: liaoyh8@mail.sysu.edu.cn

Judun Zheng: E-mail: zhengjd53815@163.com

Guangfu Liao: E-mail: liaogf@mail2.sysu.edu.cn

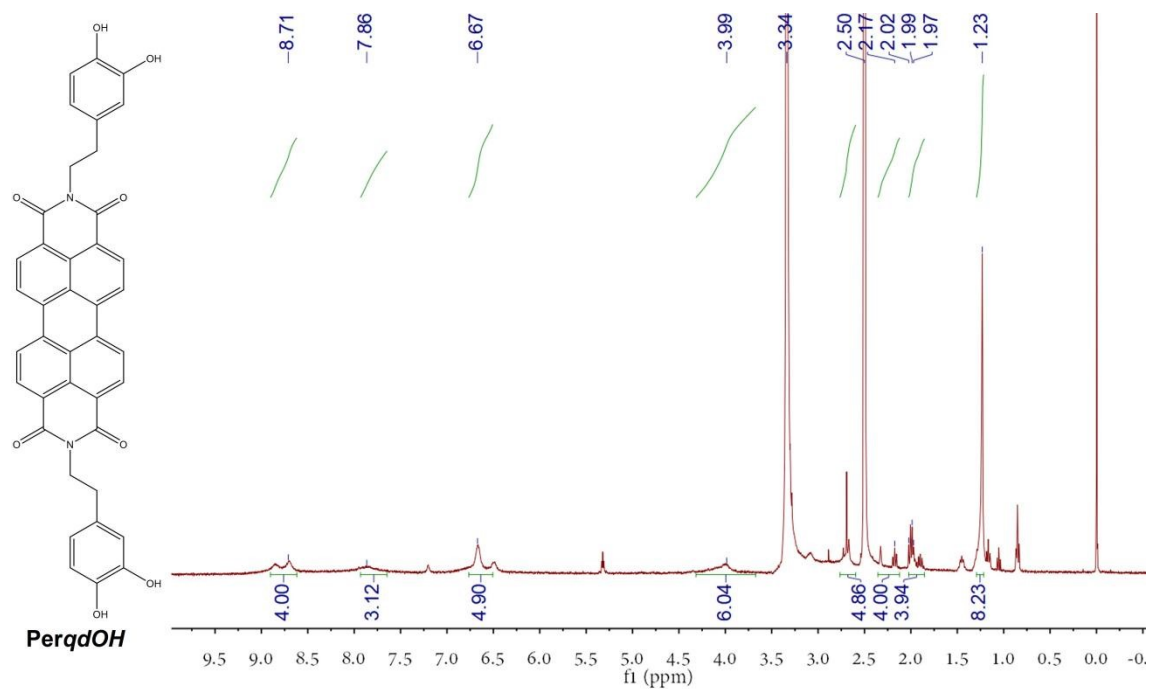


Figure S1. ^1H NMR of **PerqdOH**. ^1H NMR (400 MHz, $\text{DMSO-}d_6$) δ 8.71 (s, 4H), 7.86 (s, 3H), 6.67 (s, 5H), 3.99 (s, 6H), 2.76 – 2.59 (m, 5H), 2.17 (s, 4H), 1.98 (d, $J = 6.6$ Hz, 4H), 1.23 (s, 8H).

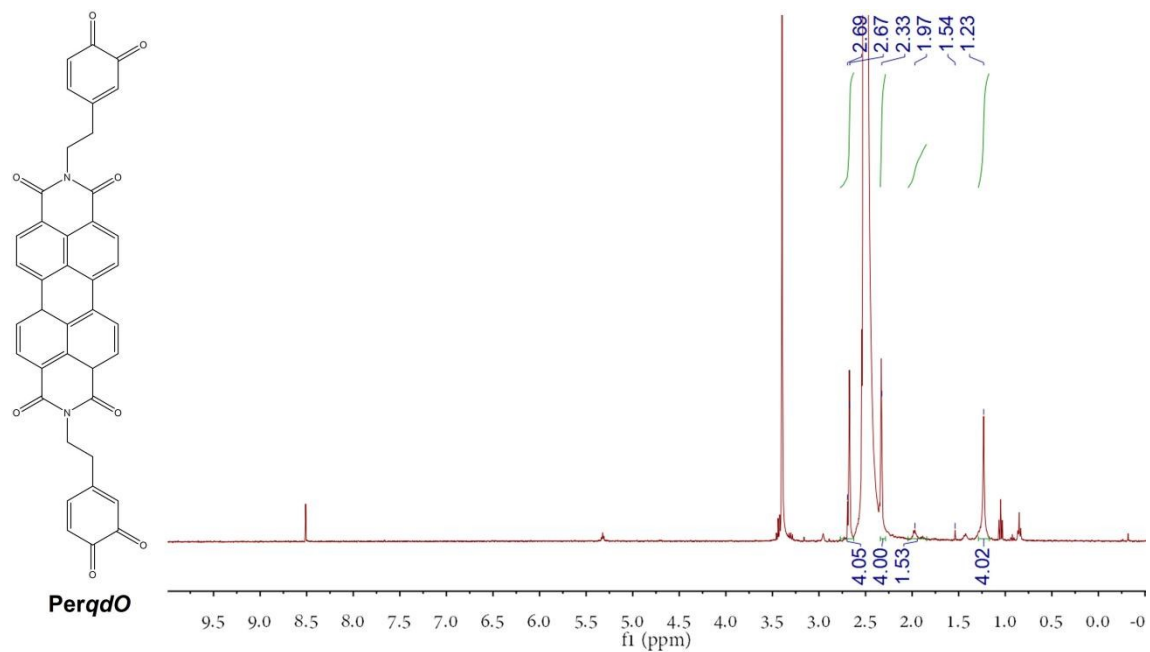


Figure S2. ^1H NMR of **PerqdO**. ^1H NMR (400 MHz, $\text{DMSO-}d_6$) δ 2.68 (d, $J = 9.6$ Hz, 4H), 2.33 (s, 4H), 1.97 (s, 2H), 1.23 (s, 4H).

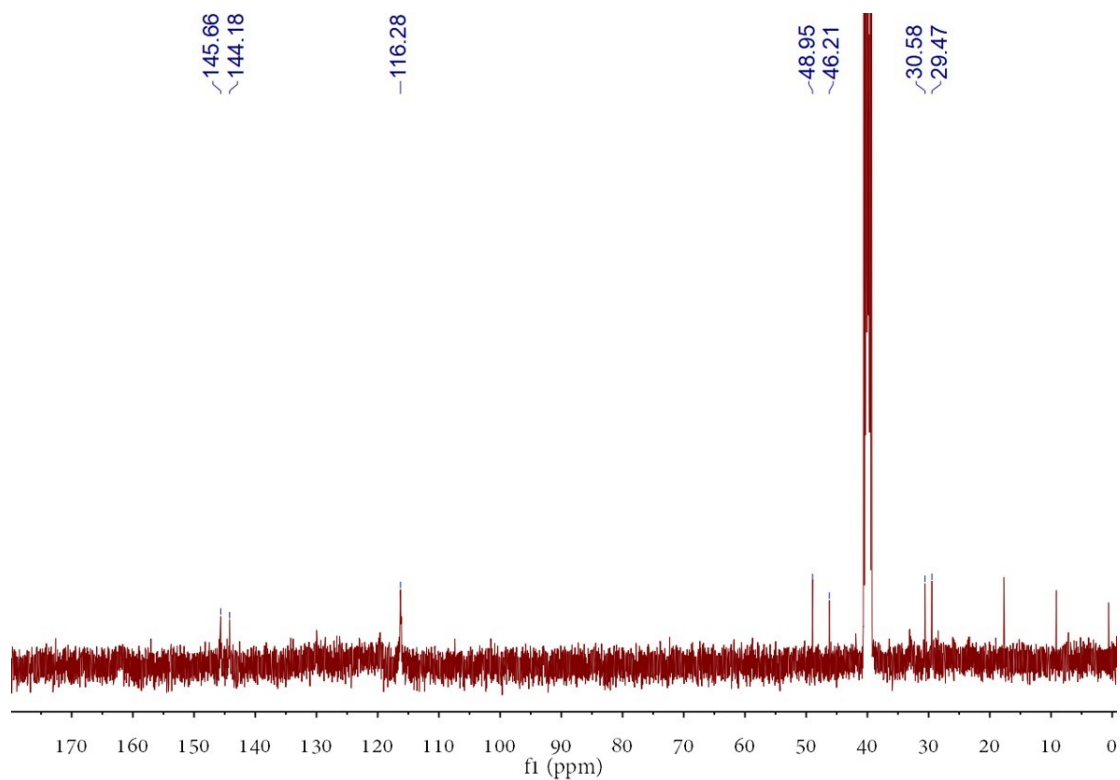


Figure S3. ¹³CNMR of *PerqdOH*. ¹³C NMR (101 MHz, DMSO-*d*₆) δ 145.66, 144.18, 116.28, 48.95, 46.21, 30.58, 29.47.

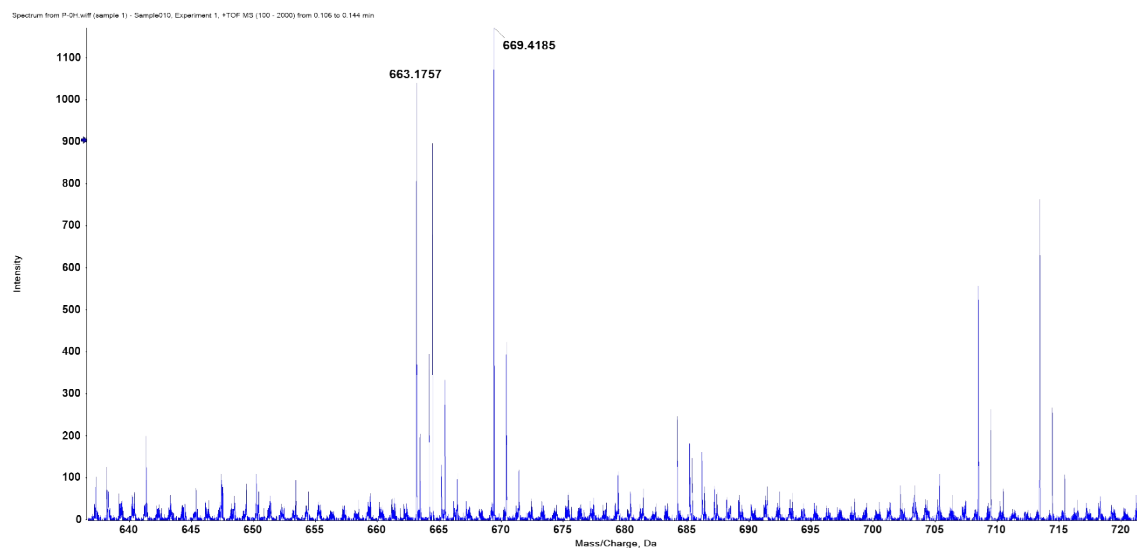


Figure S4. HR-MS of *PerqdOH*.

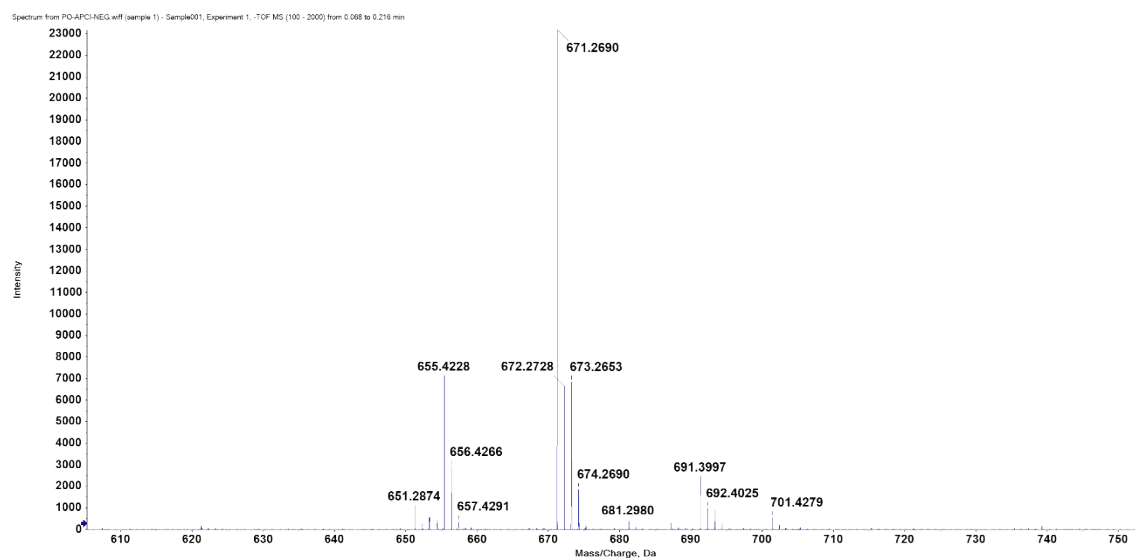


Figure S5. HR-MS of *PerqdO*.

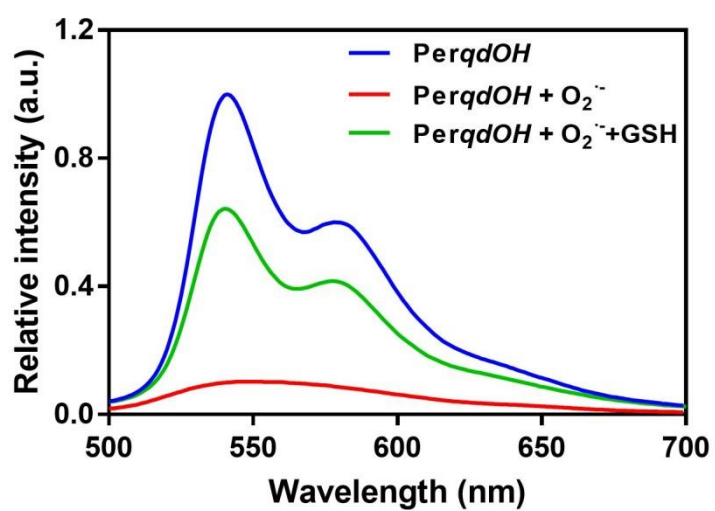


Figure S6. The fluorescence spectra change (Ex=490 nm) of *PerqdOH* after adding O₂⁻ and GSH.

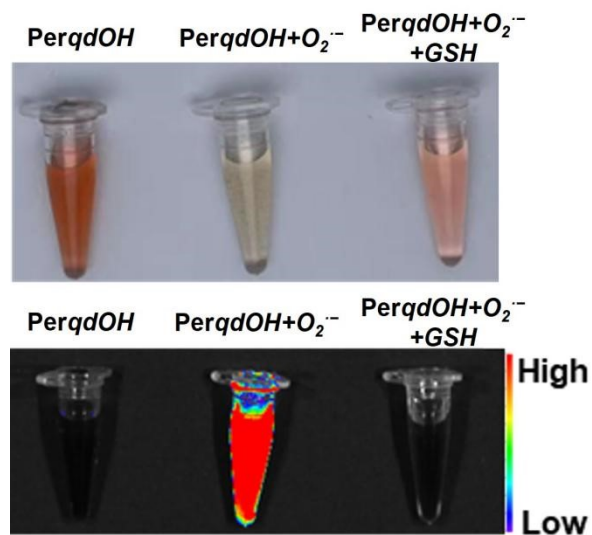


Figure S7. Images of *PerqdOH* after adding O_2^- and GSH under natural light and the condition of excitation of 680 nm and emission of 750 nm.

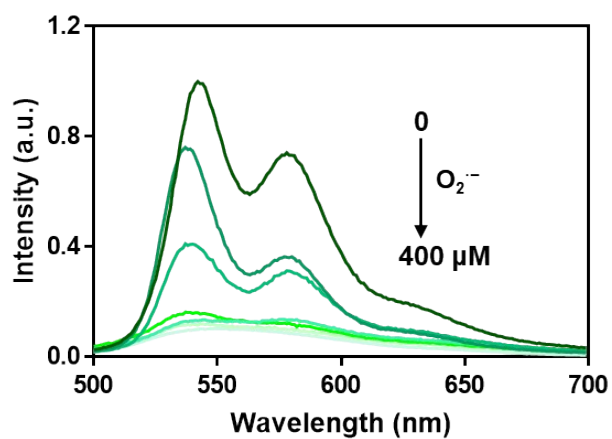


Figure S8. The fluorescence spectra change (Ex=490 nm) of *PerqdOH* after adding different concentrations of O_2^- (0-400 μ M).

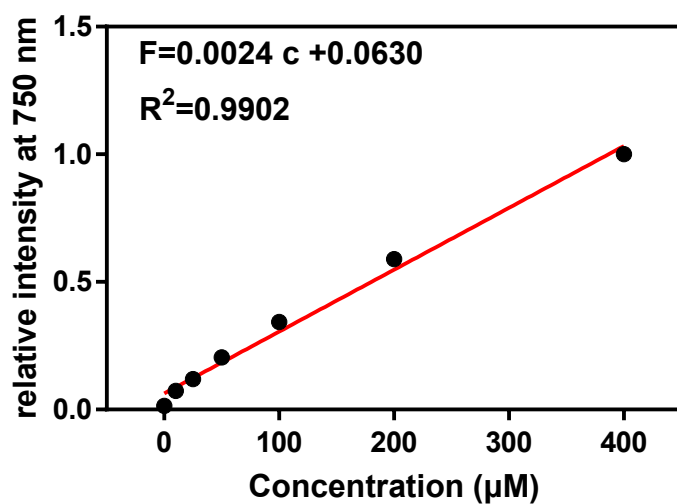


Figure S9. The linear fitting curve of the relative fluorescence intensity at 750 nm.

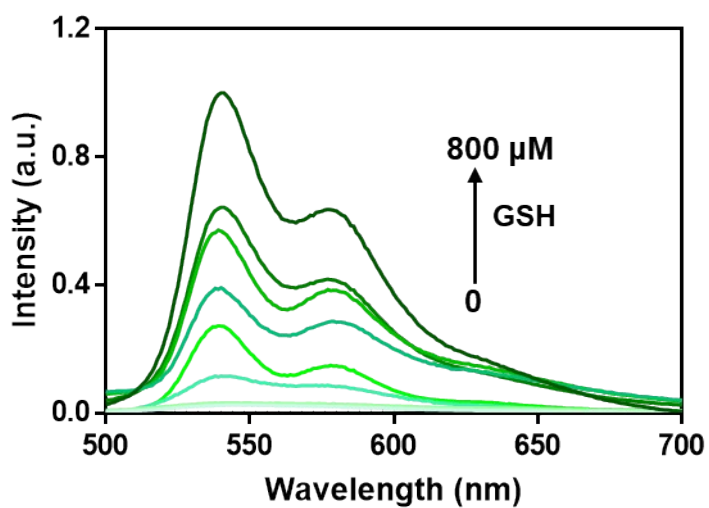


Figure S10. The fluorescence spectra change (Ex=490 nm) of *PerqDOH* after adding different concentrations of GSH (0-800 µM).

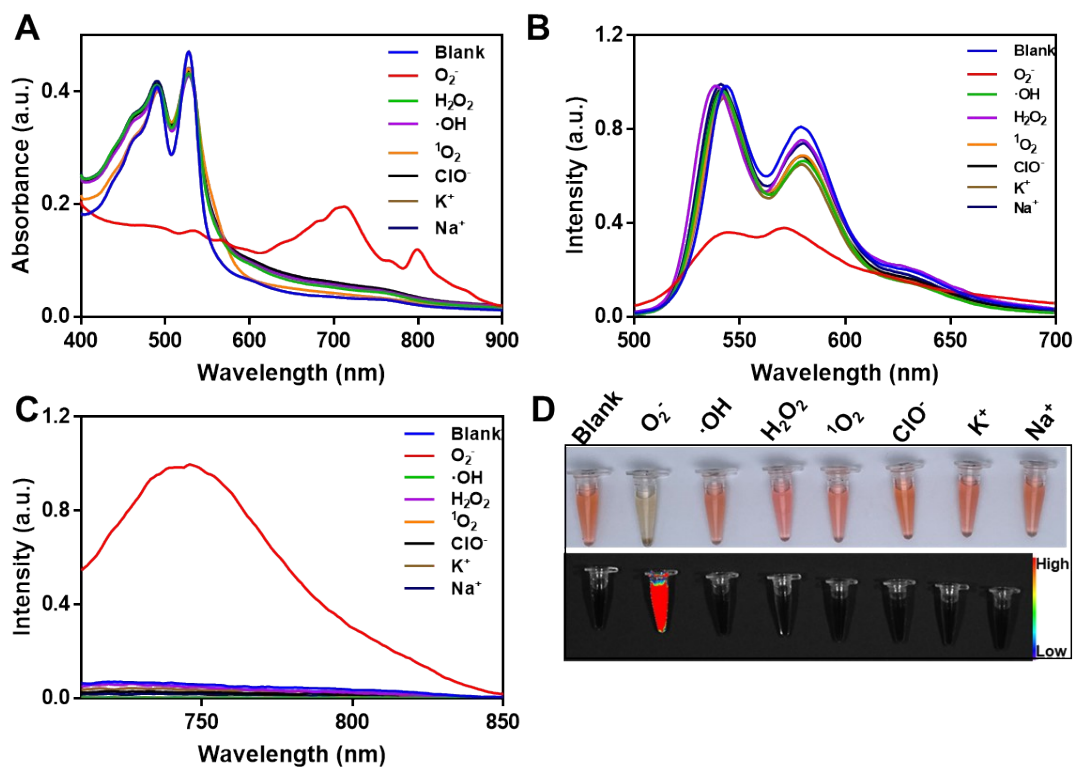


Figure S11. The selectivity of *PerqDOH* towards different ROS including O_2^- , $\cdot OH$, H_2O_2 , 1O_2 , ClO^- and so on. **A)** UV-vis spectra. Fluorescence spectra with excitation of **B)** 490 nm and **C)** 700 nm. **D)** Images of *PerqDOH* within different ROS.

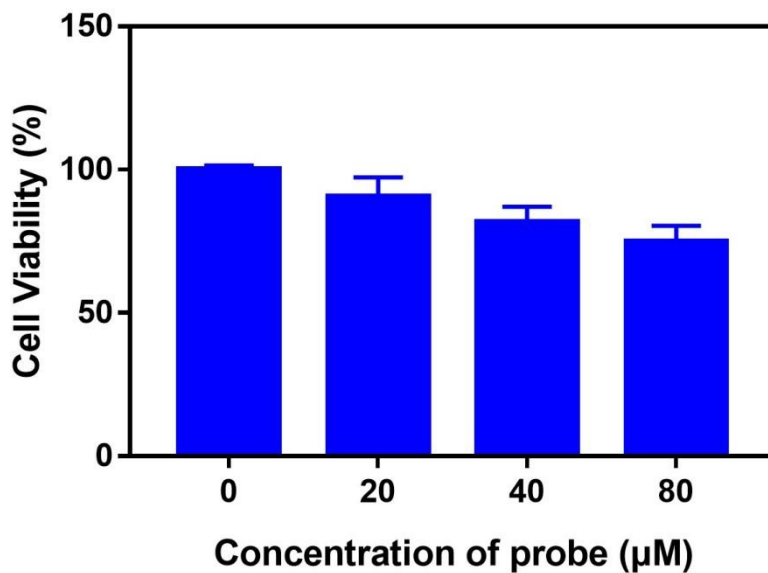


Figure S12. Cell viability under different concentration of *PerqDOH*.

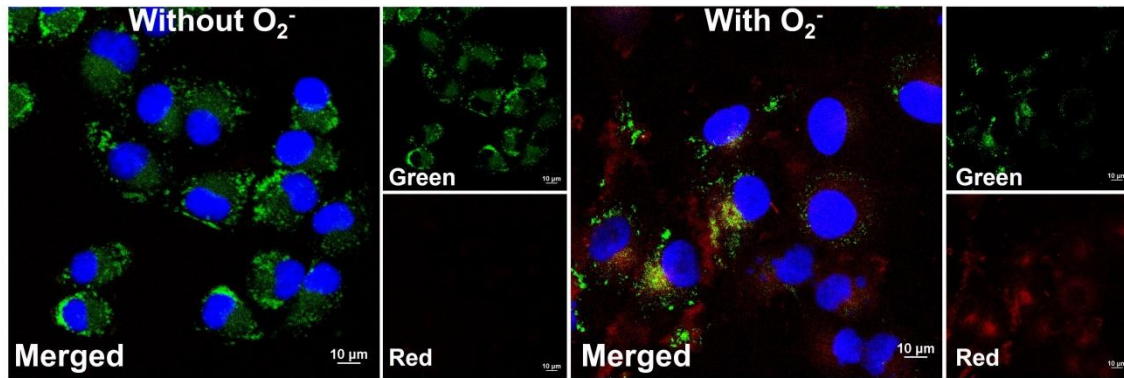


Figure S13. Fluorescence images of cell lines within and without O_2^- .

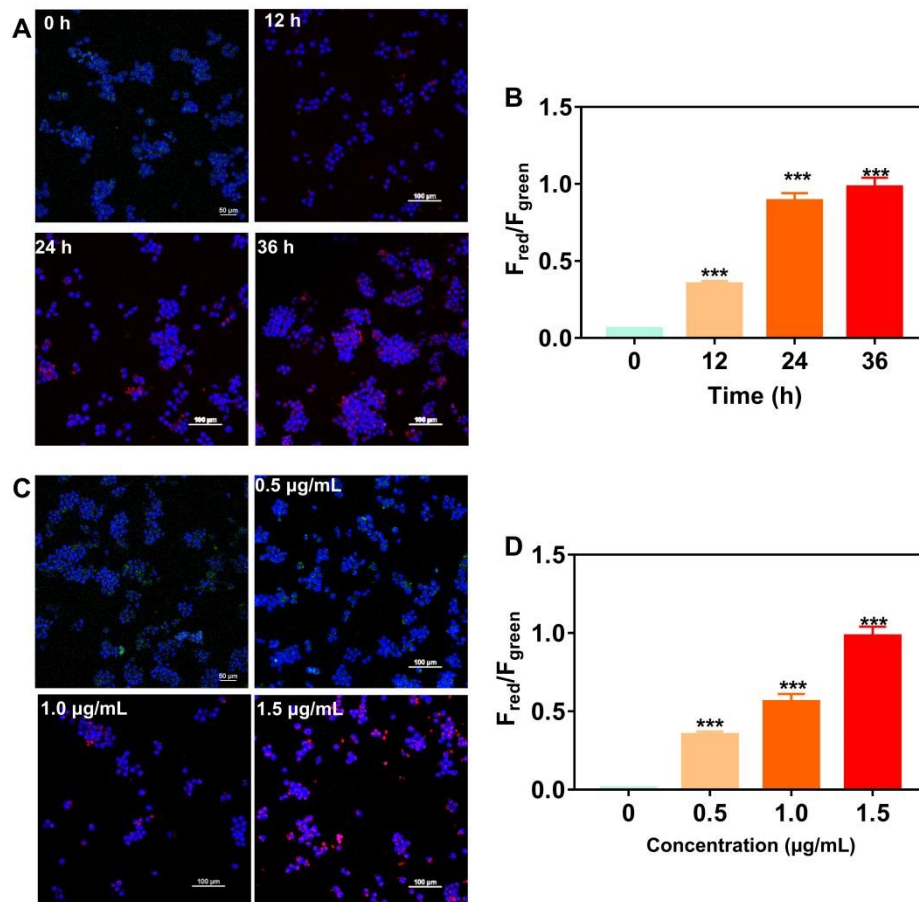


Figure S14. Monitoring endogenous O_2^- in the cells. Fluorescent images of RAW 264.7 cells after co-incubating with PMA in **A**) time-dependent manner (from 0 h to 36 h) and **B**) dose-dependent manner (0-1.5 $\mu\text{g/mL}$). **C**) and **D**) were the quantitative analysis of the relative fluorescence intensity.

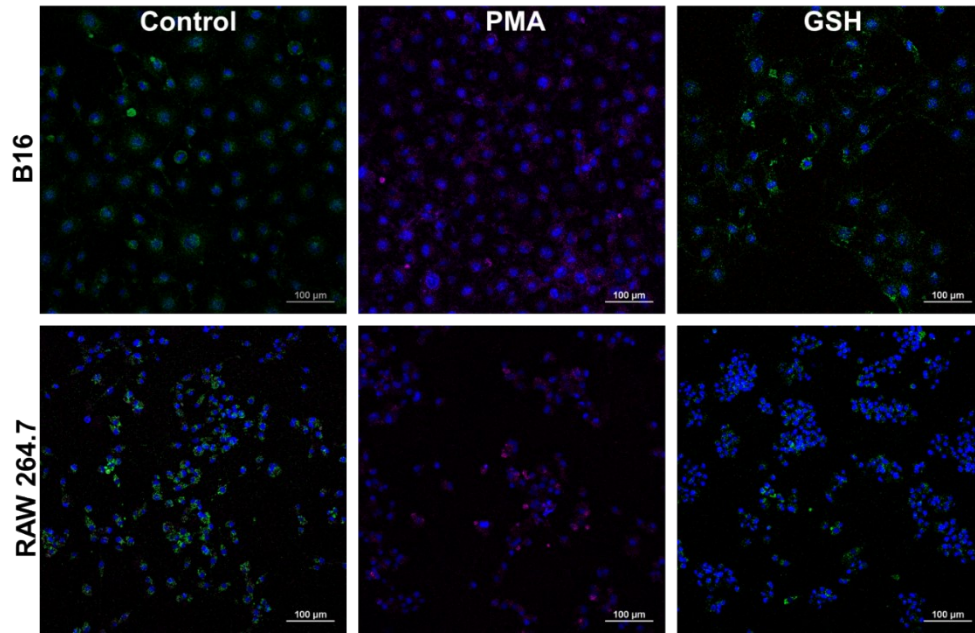


Figure S15. Fluorescence images of B16 and RAW 264.7 cell lines with the addition of PMA after pre-treating with *PerqdOH*, and the GSH was added 24 hours after the PMA was co-cultured.

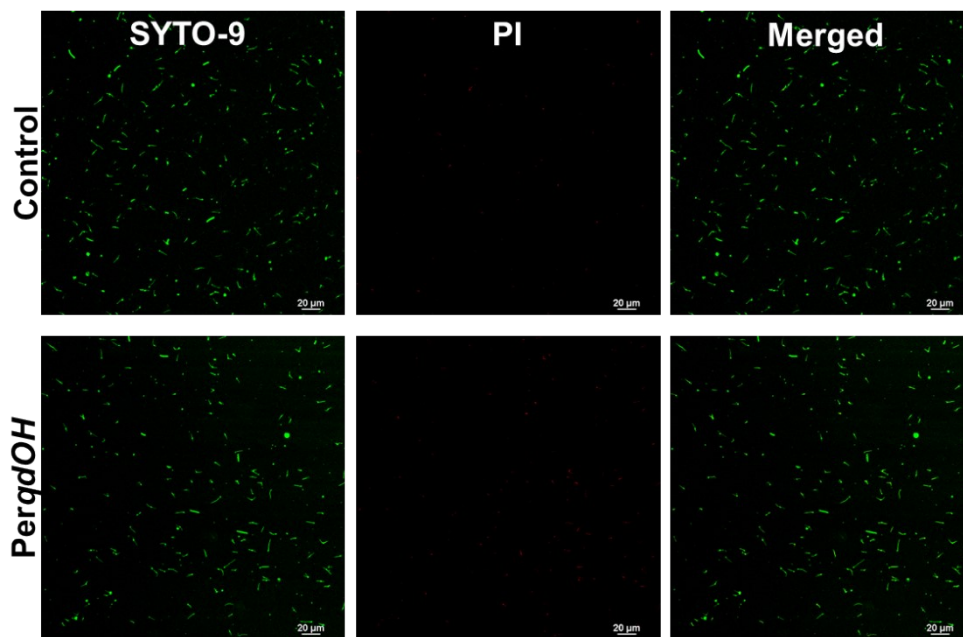


Figure S16. Toxicity evaluation of *PerqdOH* (40 μM) to the *T. pallidum*.